PCCP

Accepted Manuscript

ROYAL SOCIETY OF CHEMISTRY

www.rsc.org/pccp

The Nuclear Electric Quadrupole Moment of Copper

Régis Tadeu Santiago, Tiago Quevedo Teodoro and, Roberto Luiz Andrade Haiduke*

registsantiago@iqsc.usp.br

tiagoquevedo@iqsc.usp.br

haiduke@iqsc.usp.br

Phone 55-16-3373-8280

FAX 55-16-3373-9975

Departamento de Química e Física Molecular

Instituto de Química de São Carlos, Universidade de São Paulo

Av. Trabalhador São-carlense, 400 - CP 780

13560-970 - São Carlos, SP, Brazil

Abstract

The nuclear electric quadrupole moment (NQM) of the ^{63}Cu nucleus has been determined from an indirect approach by combining accurate experimental nuclear quadrupole coupling constants (NQCCs) with relativistic Dirac-Coulomb Coupled Cluster calculations of the electric field gradient (EFG). The data obtained at the highest level of calculation, DC-CCSD-T, from 14 linear molecules containing the copper atom give rise to an indicated NQM of -198(10) mbarn. Such result slightly deviates from the previously accepted standard value given by the muonic method, -220(15) mbarn, although the error bars are superimposed.

1. Introduction

The nuclear electric quadrupole moment (NQM) is a fundamental property that provides information about the shape of the ellipsoid of nuclear charge distribution [1]. Therefore, a positive NQM indicates a prolate spheroid whereas a negative value represents an oblate one [2].

One of the most reliable methods to determine such property is based on a combination of high level quantum chemical calculations of the electric field gradient (EFG) at a given nucleus with accurate experimental determinations of the nuclear quadrupole coupling constant (NQCC) as follows [3, 4],

$$Q(X) = \frac{\nu_Q(X)}{234.9647 q(X)}, \quad (1)$$

in which $Q(X)$, $\nu_Q(X)$ and $q(X)$ are, respectively, the NQM (in barns), the NQCC (in MHz) and the EFG (in a.u.) of an *X* nucleus in a linear molecule. This is the so-called molecular method.

However, one or both of these parameters required to NQM determinations might suffer from trivial difficulties, as the scarceness of experimental data or a high computational demand in the obtaining of results at the level of calculation needed to provide accurate NQMs. In that manner, as can be seen in a recent summary [4], some values still lack of confirmation and/or present large error bars, as occurs for copper.

Although copper is an element with many applications in ordinary chemistry [5], the NQM standard accepted value for ^{63}Cu, -220(15) mbarn, was determined more than 30 years ago by Effenberger *et al.* [6] through the muonic method. In addition, theoretical studies with common Density Functional Theory (DFT) methodologies have usually failed in describing the EFG of copper in diatomic molecules [7, 8]. However, modified functionals have been suggested in order to overwhelm this limitation. Recently, Thierfelder *et al.* [9] obtained a slightly different value for the ^{63}Cu NQM, -208 mbarn, in which the determination was based on results of a reparametrized advanced DFT method, CAM-B3LYP. A few years before, Bast and Schwerdtfeger [10] also proposed a modification of the popular B3LYP functional to deal with copper compounds and found -242 mbarn for such NQM. Hence, these two studies performed with the molecular method lead to a disagreement with the accepted NQM. Certainly, a new determination from more accurate EFG calculations can answer definitively

whether this deviation is due to the DFT methodology or the NQM currently accepted for ^{63}Cu.

In this context, we have selected 16 linear molecules containing copper, for which accurate experimental NQCC values and geometry data are available in the literature, to obtain the NQM of the ^{63}Cu nucleus through high level relativistic calculations of EFGs. This combination of NQCC and EFG data was carried out by means of a regression plot, which is derived from a procedure known as indirect approach [11-14].

2. Computational details

The calculations were done with the DIRAC12 [15] package by means of the relativistic four-component Dirac-Coulomb (DC) and Dirac-Coulomb-Gaunt (DG) Hamiltonians along with the Gaussian nuclear model. Also, (SS|SS) two-electron integrals were replaced by an interatomic correction, a procedure commonly adopted to reduce the computational demand [16]. The default speed of light value of 137.0359998 a.u. was chosen.

Sixteen linear molecules have been initially investigated: CuH, CuF, CuCl, CuBr, CuI, ArCuF, ArCuCl, ArCuBr, KrCuF, KrCuCl, XeCuF, XeCuCl, OCCuF, OCCuCl, OCCuBr and OCCuI. The calculations were performed at their equilibrium geometries experimentally determined [17-22] (these values can also be found in Table S1 of the Supplementary Material).

The Relativistic Adapted Gaussian Basis Set (RAGBS) [23] associated with the [Ar]$4s^1 3d^{10}$ configuration was chosen for the copper atom. The basis sets selected for the other atoms are indicated in Table 1 [24-27]. One can see that we used larger basis sets for the atoms bound to copper in diatomic molecules, but the increasing computational demand in larger molecules forced us to choose smaller sets for polyatomic systems. However, previous studies already demonstrated that the EFG of a particular nucleus in a molecule is usually insensitive to the basis set chosen for the remaining atoms [28, 29]. All calculations in this work used the uncontracted form of these basis sets.

Hartree-Fock (HF) and DFT (B3LYP [30, 31] and BPW91 [32, 33]) methods were used to obtain analytic EFG values, while estimates of electron correlation contributions to EFGs given by methods such as the Coupled Cluster approach with

single and double substitutions (CCSD) and its variations with perturbative triple excitation corrections [CCSD(T) and CCSD-T], which do not provide analytic EFG results in DIRAC12, were obtained by the finite-difference technique in a two point form,

$$\left(\frac{\partial E(\lambda)}{\partial \lambda}\right)_0 \approx \frac{E(+\lambda) - E(-\lambda)}{2\lambda}, \quad (2)$$

where E is the electron correlation energy and λ is the field strength, which was taken as 1×10^{-6} a.u. in order to assure more reliable energy differences compared to convergence parameters and to keep the response to the perturbation inside the linear variation regime. The active space used with this approach included all spinors with energy between -4.0 and 21.0 a.u.. Thus, from 18 to 44 electrons are inside this space depending on the molecule.

3. Results and discussion

3.1. RAGBS increment for copper

An accurate determination of the EFG at a certain nucleus depends strongly on the quality of the basis set centered at this atom. The RAGBSs are known for being free of prolapse, a common deficiency of relativistic basis sets associated to a bad description of the atomic innermost region [34], and for their success in previous EFG calculations [29, 35, 36]. However, the RAGBS for copper must be complemented with extra tight, diffuse and polarization functions to truly provide accurate EFG determinations. Thus, a study to increment the uncontracted RABGS for copper was carried out in the first step of this work by means of DC-HF and DC-B3LYP EFG calculations for this nucleus in CuH.

Hence, diffuse or tight functions of *s*, *p* or *d* symmetries were added to the original 21*s*13*p*10*d* set, one combination at a time, following a sequence with respect to the number of functions in each category. The exponents of the selected functions, which will be shown between parentheses throughout this article, were obtained by extrapolations from the polynomial Generator Coordinate Dirac-Fock (p-GCDF) [37] parameters [23]. This basis set augmentation was carried out by using a threshold of 0.0006 a.u. (approximately 0.1% of the total EFG value for copper in CuH from DC-HF or DC-B3LYP methods) for EFGs given by any of the two methods. Results are

displayed in Table 2. See that, although DC-HF and DC-B3LYP present EFGs of opposite signs, the two methods still show an overall agreement with respect to the magnitude of effects from additional functions on this property. Thus, two diffuse *p* (0.176218329 and 0.053886186), three tight *d* (1544.673985, 7586.829866 and 49266.32721) and one diffuse *d* (0.040581838) functions have been selected at this stage.

Next, a polarization study was carried out for the new 21*s*15*p*14*d* set of copper. Functions of higher angular momentum were sequentially considered and were chosen according to the same threshold previously adopted. The exponents of *l* angular momentum functions were taken from the most diffuse $l-2$ functions available in this starting set. Results are shown in Table 3. Therefore, eleven *f* (0.053886186, 0.176218329, 0.495642757, 1.234531470, 2.803644498, 5.977268485, 12.31723665, 25.25958274, 53.07782098, 117.6645633 and 283.3320087) and five *g* (0.355936877, 0.860724535, 1.918177447, 4.100733516 and 8.753812800) functions resulted in variations of the EFG above the threshold for, at least, one method and were selected to compose the augmented set of 21*s*15*p*14*d*11*f*5*g* functions.

However, as it was detailed shown by Haiduke *et al.* [36] for antimony, *p* functions with the largest exponents in a RAGBS may have to be removed from the basis set prior to its use in the finite-difference technique. Teodoro and Haiduke [35] also found some disturbances in results from this treatment associated with the tightest *d* functions of bismuth in a similar study. In that manner, we compared the EFG results of copper in CuH from DC-HF calculations obtained analytically and through the finite-difference technique. As expected, the calculations with the 21*s*15*p*14*d*11*f*5*g* set returned a considerable difference of 0.0039 a.u. between both results. After some tests, we got to a deviation (0.0001 a.u.) smaller than the threshold by withdrawing the tightest *d* function (49266.32721). Thus, the final set to be used with the finite-difference approach for copper comprises 21*s*15*p*13*d*11*f*5*g* functions, whereas the 21*s*15*p*14*d*11*f*5*g* set was employed in analytic calculations.

Although basis sets for correlated CCSD calculations must require even more functions to achieve the same accuracy in EFG determinations than those of HF and DFT results, we believe that such rigorous threshold used in the augmentation procedure (0.1 %) still assures a small error due to the basis set incompleteness.

3.2. Electric field gradients

Analytic EFG values were determined directly through DC-HF, DC-B3LYP and DC-BPW91 calculations. Results are disposed in Table 4. A further analysis of these DC-HF values showed that the 1*s* orbital of copper is responsible for 0.7 - 2.6 % of the total electronic contribution to these EFGs, whereas the sum of 2*s* and 2*p* orbitals provides 3.6 - 11.7 %. Finally, the combined effect of sub-valence 3*s* and 3*p* orbitals is more important, resulting in 8.2 - 30.4 % of this total electronic contribution. Thus, one can see that the polarization of core electrons is minor, except for the sub-valence shell.

The contributions to EFGs from correlation treatments given by high level theoretical calculations, as Second-Order Perturbation Theory (MP2) and Coupled Cluster approaches, were obtained through the finite-difference technique. However, some minor limitations are discussed.

Firstly, the full Breit term is not implemented in DIRAC12, but only part of it that is composed by the Gaunt term (DG-HF). However, Belpassi *et al.* [13] showed that this difference (gauge term) is yet not relevant for an element as heavy as gold. Moreover, Pernpointner [38] also stated that even the Gaunt-type integrals are safely negligible in EFG studies of systems containing only light elements. Hence, neglecting the gauge term is surely justifiable for copper. In addition, as can be seen from a comparison between DG-HF and DC-HF results in Table 4, the Gaunt term contributes to the analytic EFG value in only 0.8% at most.

Secondly, the limitation of the active space size (-4.0 to 21.0 a.u.) must result in a small deviation with respect to the full active space. In order to evaluate this effect, we also obtained EFGs at the DC-MP2 level by using a larger active space, in which all occupied and virtual spinors with energy up to 100 a.u. were included. The differences observed between EFG electron correlation contributions from both MP2 calculations were not larger than 3.5% of the value from the largest active space determinations. Even though, we decided to include a small correction in the final EFG values obtained by means of the Coupled Cluster approaches (Δq_{CCSD}), which is given by an equation found in Ref. [29]:

$$\Delta q_{CCSD} = \left(\frac{q_{CCSD}}{q_{MP2}} \right) \left(q_{MP2,large} - q_{MP2} \right), \quad (3)$$

in which q_{CCSD} and q_{MP2} are the electron correlation contributions to EFGs from the smallest active space in DC-CCSD [or in the variations, DC-CCSD(T) and DC-CCSD-T] and DC-MP2 calculations, whereas $q_{MP2,large}$ is the contribution to the EFG given by the largest active space in DC-MP2 results. This scaling procedure is preferable over a simple additive correction since MP2 calculations may overestimate the electron correlation contribution to EFGs in some systems [35].

Finally, the EFGs given by the DC-MP2 method (Table 4), were determined by the sum of the contribution from this electron correlation treatment to the EFGs with the analytic value determined through the DG-HF approach. The values from the DC-CCSD, DC-CCSD(T) and DC-CCSD-T methods also include the correction given by Eq. 3 in addition to the sum between analytic DG-HF results and the respective electron correlation contributions.

3.3. Nuclear quadrupole coupling constants

The NQCCs for all 16 molecules were obtained from several experimental sources [18-22, 39-41]. Since these values were measured only at the ground vibrational level (v = 0), a correction [42, 43] had to be determined to provide equilibrium NQCCs. Thus, results for the first and second derivatives of EFGs with respect to variations in bond length around the equilibrium geometry were required along with experimental molecular constants [44]. These derivatives were determined at the DC-B3LYP and DC-BPW91 levels of calculation, including four distorted geometries given by the change of ±0.005 and ±0.01Å in the equilibrium bond length. Then, by using a polynomial regression and the standard NQM of -220 mbarn, a small correction was obtained from each density functional treatment. The average of both values was summed to the NQCC given for v = 0 to obtain an estimate of equilibrium NQCCs. This procedure was applied only to the diatomic molecules. The final NQCC values are shown in Table 5 (the corrections are between parentheses). The NQCCs for the remaining molecules were not corrected in the same way because of difficulties inherent to polyatomic systems. However, given the small importance of such correction to NQCCs in these diatomic molecules, we do not expect significant changes in the determined NQMs because of this limitation.

3.4. Nuclear quadrupole moment

As explained in the Introduction section, the obtaining of an NQM value by the molecular method usually consists in the simple combination of EFG and NQCC results for a nucleus in each molecule through Eq. 1, the so-called direct approach. The results from this procedure are presented in Table 6.

Firstly, one can see that the DFT methods, B3LYP and mainly BPW91, completely fail in providing concise results. The mean absolute deviation (MAD) given by both methods is an evidence of large oscillations in the NQMs encountered for different molecules. The average NQM value by itself also differs a lot from the results determined at higher levels of calculation. The difficulties of some density functionals in properly determining EFGs have been already discussed [7-10, 45, 46].

On the other hand, although the results given by means of the DC-HF calculations are more consistent, the lack of an electron correlation treatment averages an NQM value likewise far distant from the most reliable methods. Moreover, the need for higher-order treatments of electron correlation in these diatomic molecules is evident by looking at the results of the DC-CCSD level. The huge variations are quite reduced by the inclusion of contributions from triple excitations with the perturbative DC-CCSD(T) and DC-CCSD-T approaches. In fact, absolute EFG values in these diatomic molecules are not well-described by any of these treatments, which can also be associated to the lack of a non-dynamical correlation approach [47]. This is also evidenced by the large values of the T1 diagnostic [48] obtained for CuH and CuF, 0.060 and 0.064, respectively (see Table S1 for T1 results in other molecules). Both of them are above the threshold of 0.05, recently suggested by Jiang *et al.* [49] for 3*d* transition-metal-containing molecules. Thus, since all the levels of calculation employed here are single reference methods, we decided to take both molecules out of the NQM analysis. Cheng *et al.* [47] also noticed that the full treatment of triple substitutions in CCSDT calculations may provide corrections around 10% when compared with the CCSD(T) alternative for derived NQCCs in these diatomic systems. Hence, the results of the direct approach for some of these molecules are certainly questionable.

Fortunately, another slightly different methodology has been trivially used [11-14], the indirect method, which can be more effective when a large number of molecules are available and the NQCC values show a significant spread. This indirect

approach suggests using the variation in EFG results along a molecular series instead of relying on EFG values themselves, leading to the following equation,

$$Q(X) = \frac{\Delta\nu_Q(X)}{234.9647\Delta q(X)}, \quad (4)$$

in which $\Delta\nu_Q(X)$ and $\Delta q(X)$ are, respectively, the shifts in NQCC and EFG values with respect to a reference molecule. Here, we applied this proposal by means of linear regressions (for example, see the graph in Fig. 1 constructed from DC-CCSD-T results). The NQM values given by the indirect approach are shown in Table 6 under the *regression plot* labeling. Determination and linear coefficients are given in the next lines of the same table.

The advantages of the indirect approach are noticed by the consistency among the results from different levels of calculation, which are much more efficient in predicting the EFG shifts than their absolute values. Thus, the effects from higher-order electron correlation treatments than the ones considered here are quite reduced by an indirect determination once some cancelation is readily expected in the case of EFG shifts. For example, while the oscillations seen in the NQMs of different molecules with the density functional and the direct procedure lead to averages of 780 and -398 mbarn, the indirect approach, based on the same results, provides values in reasonable accordance with the ones from more advanced levels. This improvement is also evident in DC-HF results. On the other hand, it is now clear by the non-vanishing intercepts that HF, DFT and CCSD (without triple contributions) methodologies present some sort of systematic error. It is also noticeable that DC-MP2 tends to overcorrect the electron correlation effect on these indirect NQM values as one compares the tendency from DC-HF to DC-CCSD(T) or DC-CCSD-T results. Moreover, the points associated with DC-MP2 are also more disperse than those from the highest levels. DC-CCSD results are still somewhat far away from those of treatments with triple excitations, which is not totally surprising taking into account that a smaller than 0.05 T1 value still may indicate possible problematic cases when triple excitations are not included [49].

Therefore, we obtained NQM values of -199 and -198 mbarn by means of linear regressions with the EFGs obtained at the highest levels, DC-CCSD(T) and DC-CCSD-T, respectively. Both results are virtually the same and deviate from the respective ones given by the direct method in only 4%. Moreover, alternative

regressions from the same electronic structure treatments that go through the origin, which were used to further evaluate the error estimate, also provided a similar value, -203 mbarn.

Another procedure that could be used to attest the indirect determination is to identify those molecules in which the single reference approach is more successful and take their direct results as comparison. This can be assessed by searching for the smallest differences between direct NQM determinations at DC-CCSD and DC-CCSD(T) or DC-CCSD-T methods, which should indicate to those molecules less sensitive to higher order effects of correlation treatments on EFGs. This analysis clearly shows that OCCuX (X=F, Cl, Br and I) systems are better fitted to a direct approach, leading to an average NQM of -202 mbarn from both DC-CCSD(T) and DC-CCSD-T levels. Besides, the coefficient of determination from both levels (0.999), in addition to their very small *intercept* values, endorses the reliability of our study.

Finally, by selecting the indirect results from the highest level of calculation addressed here, DC-CCSD-T, and considering the possible error sources that may persist, such as those attributed to any remaining basis set incompleteness effects, the lack of higher-order treatments of electron correlation or the neglecting of other quantum electrodynamical effects [28, 36], we indicate an NQM value for the ^{63}Cu nucleus of -198(10) mbarn. The assumed error was maintained in a conservative value of 5% due also to the particular difficulties found in the electron correlation treatment for some of these copper containing molecules.

4. Conclusions

The results from DC-CCSD-T calculations for the EFG at the copper nuclei in 14 molecules, in addition to accurate experimental NQCC data, led us to a proposed NQM of -198(10) mbarn for ^{63}Cu. This value was determined by means of an indirect approach through a linear regression plot ($R^2 = 0.999$).

Such result slightly deviates from the previously accepted standard value, -220(15) mbarn [6]. However, considering the high level of these EFG calculations and the accuracy of the NQCCs used in our study, associated to the robust indirect approach with a large number of molecules, we suggest a revision of the currently accepted value.

Acknowledgments

The authors acknowledge FAPESP for financial support during the development of this work (Grant No. 2010/18743-1). TQT also thanks FAPESP for a doctoral fellowship (Grant No. 2012/22143-5). RTS acknowledges CAPES for a Master's fellowship.

References

1. G. Neyens, *Rep. Prog. Phys.*, 2003, **66**, 633-689.
2. *Pure and Applied Chemistry*, 1976, **45**, 211-216.
3. P. Pyykkö, *Mol. Phys.*, 2001, **99**, 1617-1629.
4. P. Pyykkö, *Mol. Phys.*, 2008, **106**, 1965-1974.
5. H. W. Richardson, Handbook of copper compounds and applications, New York: M. Dekker, 1997.
6. B. Effenberger, W. Kunold, W. Oesterle, M. Schneider, L. M. Simons, R. Abela and J. Wuest, *Z. Phys. A-Hadron. Nucl.*, 1982, **309**, 77-81.
7. P. Schwerdtfeger, M. Pernpointner and J. K. Laerdahl, *J. Chem. Phys.*, 1999, **111**, 3357-3364.
8. M. Srebro and J. Autschbach, *J. Phys. Chem. Lett.*, 2012, **3**, 576-581.
9. C. Thierfelder, P. Schwerdtfeger and T. Saue, *Phys. Rev. A*, 2007, **76**, 034502.
10. R. Bast and P. Schwerdtfeger, *J. Chem. Phys.*, 2003, **119**, 5988-5994.
11. P. Dufek, P. Blaha and K. Schwarz, *Phys. Rev. Lett.*, 1995, **75**, 3545-3548.
12. P. Schwerdtfeger, R. Bast, M. C. L. Gerry, C. R. Jacob, M. Jansen, V. Kellö, A. V. Mudring, A. J. Sadlej, T. Saue, T. Söhnel and F. E. Wagner, *J. Chem. Phys.*, 2005, **122**, 124317.
13. L. Belpassi, F. Tarantelli, A. Sgamellotti, H. M. Quiney, J. N. P. van Stralen and L. Visscher, *J. Chem. Phys.*, 2007, **126**, 064314.
14. L. Belpassi, F. Tarantelli, A. Sgamellotti, A. W. Götz and L. Visscher, *Chem. Phys. Lett.*, 2007, **442**, 233-237.
15. DIRAC, a relativistic ab initio electronic structure program, Release DIRAC12 (2012), written by H. J. Aa. Jensen, R. Bast, T. Saue, and L. Visscher, with contributions from V. Bakken, K. G. Dyall, S. Dubillard, U. Ekström, E. Eliav, T. Enevoldsen, T. Fleig, O. Fossgaard, A. S. P. Gomes, T. Helgaker, J. K. Lærdahl, Y. S. Lee, J. Henriksson, M. Iliaš, Ch. R. Jacob, S. Knecht, S. Komorovský, O. Kullie, C. V. Larsen, H. S. Nataraj, P. Norman, G. Olejniczak, J. Olsen, Y. C. Park, J. K. Pedersen, M. Pernpointner, K. Ruud, P. Sałek, B. Schimmelpfennig, J. Sikkema, A. J. Thorvaldsen, J. Thyssen, J. van Stralen, S. Villaume, O. Visser, T. Winther, and S. Yamamoto (see http://www.diracprogram.org).
16. L. Visscher, *Theor. Chem. Acc.*, 1997, **98**, 68-70.

17. K. P. Huber and G. Herzberg, Molecular Spectra and Molecular Structure Constants, New York: Van Nostrand, 1979.
18. C. J. Evans and M. C. L. Gerry, *J. Chem. Phys.*, 2000, **112**, 9363-9374.
19. J. M. Michaud, S. A. Cooke and M. C. L. Gerry, *Inorg. Chem*, 2004, **43**, 3871-3881.
20. J. M. Michaud and M. C. L. Gerry, *J. Am. Chem. Soc.*, 2006, **128**, 7613-7621.
21. N. R. Walker and M. C. L. Gerry, *Inorg. Chem*, 2001, **40**, 6158-6166.
22. S. G. Batten and A. C. Legon, *Chem. Phys. Lett.*, 2006, **422**, 192-197.
23. R. L. A. Haiduke and A. B. F. da Silva, *J. Comput. Chem*, 2006, **27**, 61-71.
24. D. E. Woon and T. H. Dunning, *J. Chem. Phys.*, 1993, **98**, 1358-1371.
25. T. H. Dunning, *J. Chem. Phys.*, 1989, **90**, 1007-1023.
26. K. G. Dyall, *Theor. Chem. Acc.*, 1998, **99**, 366-371. Addendum K. G. Dyall, *Theor. Chem. Acc.*, 2002, **108**, 365-365. Revision K. G. Dyall, *Theor. Chem. Acc.*, 2006, **115**, 441-447.
27. K. G. Dyall, *Theor. Chem. Acc.*, 2002, **108**, 335-340. Revision K. G. Dyall, *Theor. Chem. Acc.*, 2006, **115**, 441-447.
28. J. N. P. van Stralen and L. Visscher, *J. Chem. Phys.*, 2002, **117**, 3103-3108.
29. R. L. A. Haiduke, *Chem. Phys. Lett.*, 2012, **544**, 13-16.
30. A. D. Becke, *J. Chem. Phys.*, 1993, **98**, 5648-5652.
31. P. J. Stephens, F. J. Devlin, C. F. Chabalowski and M. J. Frisch, *J. Phys. Chem-Us*, 1994, **98**, 11623-11627.
32. J. P. Perdew and Y. Wang, *Phys. Rev. B*, 1992, **45**, 13244-13249.
33. A. D. Becke, *Phys. Rev. A*, 1988, **38**, 3098-3100.
34. H. Tatewaki and Y. Watanabe, *J. Chem. Phys.*, 2004, **121**, 4528-4533.
35. T. Q. Teodoro and R. L. A. Haiduke, *Phys. Rev. A*, 2013, **88**, 052504.
36. R. L. A. Haiduke, A. B. F. da Silva and L. Visscher, *J. Chem. Phys.*, 2006, **125**, 064301.
37. R. L. A. Haiduke, L. G. M. De Macedo, R. C. Barbosa and A. B. F. Da Silva, *J. Comput. Chem*, 2004, **25**, 1904-1909.
38. M. Pernpointner, *J. Phys. B: At. Mol. Opt. Phys.*, 2002, **35**, 383-394.
39. T. Okabayashi and M. Tanimoto, *Astrophys. J.*, 1997, **487**, 463-465.
40. R. J. Low, T. D. Varberg, J. P. Connelly, A. R. Auty, B. J. Howard and J. M. Brown, *J. Mol. Spectrosc.*, 1993, **161**, 499-510.
41. S. G. Batten, A. G. Ward and A. C. Legon, *J. Mol. Struct.*, 2006, **780-81**, 300-305.
42. J. N. P. Van Stralen and L. Visscher, *Mol. Phys.*, 2003, **101**, 2115-2124.
43. M. Seth, M. Pernpointner, G. A. Bowmaker and P. Schwerdtfeger, *Mol. Phys.*, 1999, **96**, 1767-1780.
44. D. R. Lide, "Spectroscopic Constants of Diatomic Molecules in CRC Handbook of Chemistry and Physics 94th edn," Boca Raton, FL, (Internet Version 2014) ed Haynes W. M. CRC Press/Taylor and Francis: , http://www.hbcpnetbase.com/
45. E. van Lenthe and E. J. Baerends, *J. Chem. Phys.* 2000, **112**, 8279-8292.

46. P. Schwerdtfeger, T. Söhnel, M. Pernpointner, J. K. Laerdahl and F. E. Wagner, *J. Chem. Phys.*, 2001, **115**, 5913-5924.
47. L. Cheng, S. Stopkowicz, J. F. Stanton and J. Gauss, *J. Chem. Phys*, 2012, **137**, 224302.
48. T. J. Lee and P. R. Taylor, *Int. J. Quant. Chem.*, 1989, 199-207.
49. W. Jiang, N. J. DeYonker and A. K. Wilson, *J. Chem. Theory Comput.*, 2012, **8**, 460-468.

Table 1 – Basis sets selected for the EFG calculations.

(Y-Cu-X)[a]	Y	X
CuH	-	cc-pVQZ
CuF	-	cc-pVQZ
CuCl	-	cc-pVQZ
CuBr	-	dyall.cv3z
CuI	-	dyall.cv3z
ArCuF	cc-pVTZ	cc-pVTZ
ArCuCl	cc-pVTZ	cc-pVTZ
ArCuBr	cc-pVTZ	dyall.cv3z
KrCuF	dyall.cv3z	cc-pVTZ
KrCuCl	dyall.cv3z	cc-pVTZ
XeCuF	dyall.cv2z	cc-pVTZ
XeCuCl	dyall.cv2z	cc-pVTZ
OCCuF	cc-pVTZ	cc-pVTZ
OCCuCl	cc-pVTZ	cc-pVTZ
OCCuBr	cc-pVTZ	dyall.cv2z
OCCuI	cc-pVTZ	dyall.cv2z

[a] X refers to hydrogen or an halogen while Y is a noble gas or the C, O pair of atoms.

Table 2 – EFGs (a.u.) at the Cu nucleus in the CuH[a] molecule obtained during a basis set convergence study with the addition of tight and diffuse functions.

Basis set	DC-HF		DC-B3LYP	
	q	Δq	q	Δq
21*s*13*p*10*d*[b]	-0.5654		0.5630	
+1 tight *s*	-0.5654	0.0000	0.5630	0.0000
+2 tight *s*	-0.5654	0.0000	0.5630	0.0000
+1 tight *p*	-0.5659	-0.0005	0.5628	-0.0002
+2 tight *p*	-0.5660	-0.0001	0.5628	0.0000
+1 tight *d*[c]	-0.5855	-0.0201	0.5417	-0.0213
+2 tight *d*[c]	-0.5894	-0.0039	0.5359	-0.0058
+3 tight *d*[c]	-0.5909	-0.0014	0.5345	-0.0014
+4 tight *d*	-0.5913	-0.0004	0.5340	-0.0005
+5 tight *d*	-0.5914	-0.0001	0.5338	-0.0002
+1 diffuse *s*	-0.5654	0.0000	0.5630	0.0000
+1 diffuse *p*[c]	-0.5703	-0.0049	0.5617	-0.0013
+2 diffuse *p*[c]	-0.5732	-0.0028	0.5599	-0.0018
+3 diffuse *p*	-0.5730	0.0002	0.5598	-0.0001
+1 diffuse *d*[c]	-0.5664	-0.0010	0.5565	-0.0065
+2 diffuse *d*	-0.5664	0.0000	0.5564	-0.0001
21*s*15*p*14*d*[d]	-0.5988	-0.0334	0.5262	-0.0368

[a] cc-pVQZ basis set for the H atom;
[b] Original RAGBS for the copper atom;
[c] Selected functions;
[d] RAGBS incremented with the selected functions.

Table 3 – EFGs (a.u.) at the Cu nucleus in the CuH[a] molecule obtained during a basis set convergence study with the addition of polarization functions.

Basis set	DC-HF		DC-B3LYP	
	q	Δq	q	Δq
21s15p14d	-0.5988		0.5262	
+ 1f[b]	-0.6001	-0.0013	0.5253	-0.0009
+ 2f[b]	-0.6172	-0.0171	0.5119	-0.0134
+ 3f[b]	-0.6612	-0.0440	0.4756	-0.0363
+ 4f[b]	-0.6765	-0.0153	0.4578	-0.0178
+ 5f[b]	-0.6830	-0.0066	0.4493	-0.0085
+ 6f[b]	-0.6836	-0.0005	0.4467	-0.0026
+ 7f[b]	-0.6813	0.0023	0.4440	-0.0028
+ 8f[b]	-0.6829	-0.0016	0.4364	-0.0075
+ 9f[b]	-0.6872	-0.0043	0.4275	-0.0090
+ 10f[b]	-0.6881	-0.0009	0.4248	-0.0027
+ 11f[b]	-0.6882	-0.0001	0.4242	-0.0006
+ 12f	-0.6882	0.0000	0.4242	0.0000
21s15p14d11f	-0.6882		0.4242	
+ 1g	-0.6882	0.0000	0.4242	0.0000
+ 2g	-0.6882	0.0000	0.4242	-0.0001
+ 3g[b]	-0.6891	-0.0008	0.4241	-0.0013
+ 4g[b]	-0.6938	-0.0048	0.4228	-0.0058
+ 5g[b]	-0.6957	-0.0019	0.4170	-0.0035
+ 6g[b]	-0.6957	0.0000	0.4135	-0.0014
+ 7g[b]	-0.6955	0.0002	0.4121	-0.0009
+ 8g	-0.6957	-0.0002	0.4111	-0.0002
21s15p14d11f5g[c]	-0.6956		0.4111	
+ 1h	-0.6956	0.0000	0.4111	0.0000
+ 2h	-0.6956	0.0000	0.4111	0.0000
+ 3h	-0.6955	0.0001	0.4112	0.0002

[a] cc-pVQZ basis set for the H atom;
[b] Selected functions;
[c] Basis set obtained after the polarization study.

Table 4 – EFGs (in a.u.) at the Cu nuclei given by different theoretical treatments.

Molecules	DC-HF[a]	DG-HF[a]	DC-BPW91[a]	DC-B3LYP[a]	DC-MP2[b]	DC-MP2[c]	DC-CCSD[d]	DC-CCSD(T)[d]	DC-CCSD-T[d]
CuH	-0.696	-0.697	0.638	0.411	-0.084	-0.066	0.175	-0.010	-0.006
CuF	-1.298	-1.302	0.746	0.314	-0.462	-0.445	0.225	-0.495	-0.501
CuCl	-0.893	-0.895	0.577	0.263	-0.383	-0.379	-0.027	-0.349	-0.344
CuBr	-0.750	-0.751	0.562	0.279	-0.324	-0.323	0.014	-0.253	-0.250
CuI	-0.578	-0.578	0.520	0.287	-0.226	-0.225	0.047	-0.139	-0.139
ArCuF	-1.490	-1.495	0.124	-0.169	-0.641	-0.619	-0.650	-0.778	-0.771
ArCuCl	-1.210	-1.213	0.064	-0.171	-0.644	-0.639	-0.538	-0.674	-0.668
ArCuBr	-1.093	-1.095	0.086	-0.136	-0.607	-0.606	-0.469	-0.609	-0.604
KrCuF	-1.535	-1.540	0.014	-0.273	-0.738	-0.719	-0.724	-0.861	-0.855
KrCuCl	-1.254	-1.257	-0.040	-0.266	-0.725	-0.719	-0.624	-0.749	-0.744
XeCuF	-1.605	-1.610	-0.436	-0.157	-0.899	-0.883	-0.868	-1.004	-0.999
XeCuCl	-1.317	-1.320	-0.194	-0.409	-0.866	-0.860	-0.773	-0.882	-0.878
OCCuF	-2.220	-2.224	-0.845	-1.095	-1.095	-1.482	-1.461	-1.553	-1.594
OCCuCl	-2.012	-2.014	-0.856	-1.062	-1.062	-1.450	-1.437	-1.457	-1.497
OCCuBr	-1.919	-1.921	-0.808	-1.008	-1.008	-1.394	-1.384	-1.369	-1.419
OCCuI	-1.817	-1.819	-0.783	-0.973	-0.973	-1.352	-1.344	-1.300	-1.354

[a]Analytic EFG values;
[b] Sum of the DG-HF EFG value with the electron correlation contribution obtained with a larger active space;
[c] Sum of the DG-HF EFG value with the electron correlation contribution;
[d] Sum of the DG-HF EFG value with the electron correlation contribution obtained by the respective method plus the correction given by Eq. 3.

Table 5 – NQCCs (in MHz) at the ^{63}Cu nuclei.

Molecule	NQCC
CuH[a,b]	0.45 (-0.39)
CuF[a,c]	21.72 (-0.24)
CuCl[a,d]	16.06 (-0.11)
CuBr[a,d]	12.77 (-0.08)
CuI[a,e]	7.84 (-0.06)
ArCuF[c]	75.41
ArCuCl[c]	70.83
ArCuBr[c]	67.53
KrCuF[f]	64.50
KrCuCl[f]	38.05
XeCuF[g]	33.19
XeCuCl[g]	29.92
OCCuF[h]	41.77
OCCuCl[h]	36.52
OCCuBr[h]	47.76
OCCuI[i]	41.57

[a] Equilibrium corrected values (vibrational corrections are between parentheses, see Section 3.3. for details);
[b] Ref. [39];
[c] Ref. [18];
[d] Ref. [40];
[e] Ref. [41];
[f] Ref. [19];
[g] Ref. [20];
[h] Ref. [21];
[i] Ref. [22].

Table 6 – NQMs of the ^{63}Cu nuclei (in mbarn) determined through various theoretical treatment levels.

Molecules	DC-HF	DG-HF	DC-BPW91	DC-B3LYP	DC-MP2[a]	DC-MP2	DC-CCSD	DC-CCSD(T)	DC-CCSD-T
CuH	-2.8	-2.8	3.0	4.7	-22.8	-29.1	11.0	-189.0	-330.2
CuF	-71.2	-71.0	123.9	294.2	-199.9	-207.5	410.3	-186.8	-184.6
CuCl	-76.5	-76.4	118.5	259.7	-178.5	-180.6	-2544.7	-195.7	-198.6
CuBr	-72.4	-72.3	96.6	194.8	-168.0	-168.2	3809.4	-214.8	-217.0
CuI	-57.7	-57.7	64.1	116.1	-147.5	-148.0	707.9	-240.2	-240.3
ArCuF	-108.7	-108.3	1307.1	-958.6	-252.8	-261.7	-249.3	-208.3	-210.1
ArCuCl	-116.7	-116.4	2221.2	-828.0	-219.4	-221.2	-262.4	-209.7	-211.4
ArCuBr	-116.5	-116.3	1476.8	-937.0	-209.7	-210.3	-271.6	-209.2	-210.9
KrCuF	-115.8	-115.4	12975.4	-650.0	-240.8	-247.4	-245.5	-206.4	-207.8
KrCuCl	-124.0	-123.7	-3860.4	-584.8	-214.5	-216.1	-249.0	-207.5	-208.8
XeCuF	-126.6	-126.3	-466.6	-1292	-226.0	-230.2	-234.2	-202.4	-203.4
XeCuCl	-134.3	-134.0	-912.1	-432.3	-204.3	-205.6	-229.0	-200.7	-201.4
OCCuF	-144.6	-144.3	-380.0	-293.2	-216.5	-219.7	-206.7	-201.3	-200.9
OCCuCl	-149.8	-149.7	-352.1	-283.9	-208.0	-209.8	-207.0	-201.4	-201.3
OCCuBr	-149.8	-149.6	-355.7	-285.1	-206.2	-207.6	-210.0	-202.5	-202.4
OCCuI	-151.1	-150.9	-350.6	-282.2	-203.1	-204.3	-211.2	-202.8	-202.5
Average[b]	**-114.4**	**-114.2**	**780.4**	**-397.5**	**-206.3**	**-209.2**	**-12.9**	**-206.0**	**-206.8**
MAD[b,c]	24.7	24.7	1981.2	386.7	18.3	19.0	662.1	7.2	7.9
Regression plot[b,d]	**-187.0**	**-186.6**	**-171.8**	**-180.2**	**-214.0**	**-215.4**	**-171.8**	**-199.0**	**-198.2**
R^{2} [b,d]	0.972	0.971	0.961	0.947	0.980	0.976	0.996	0.999	0.999
Intercept (MHz)[b,d]	-20.13	-20.12	35.89	26.91	-0.43	-0.23	12.03	1.07	1.36

[a] Values obtained by using EFG results determined with a larger active space (See Section 3.2.);
[b] These values do not include results for CuH and CuF molecules due the high T1 diagnostic values detected;
[c] Mean absolute deviation;
[d] Results determined through an indirect approach (see Section 3.4).

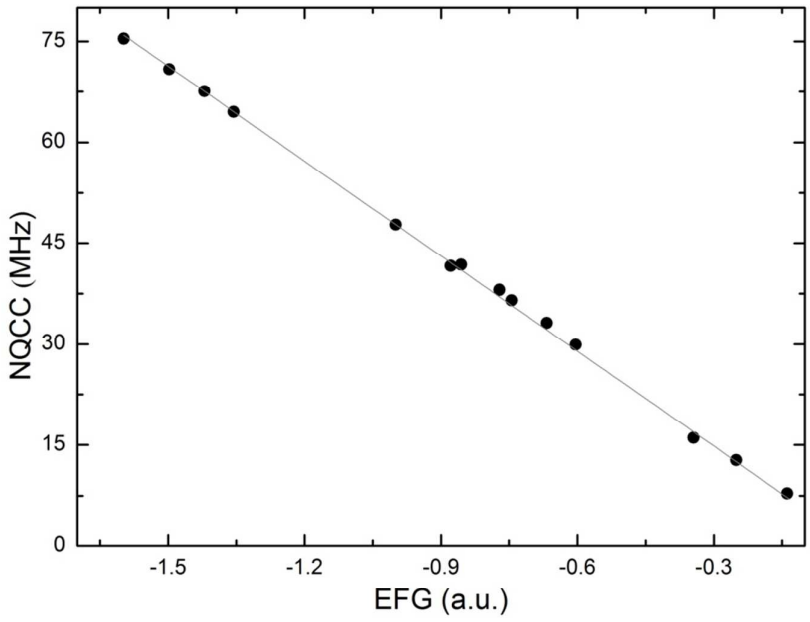

Figure 1 – Regression plot of experimental NQCC results against EFG values calculated at the DC-CCSD-T level for the 14 molecules selected in this study.

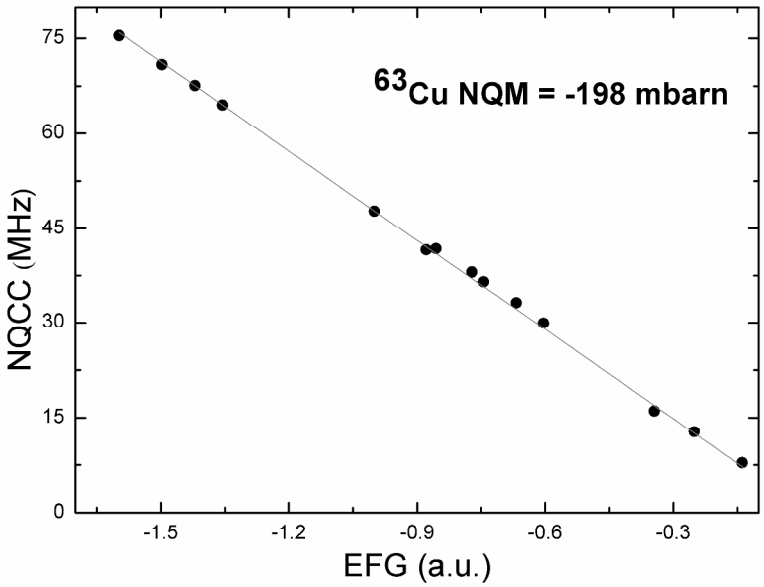

289x203mm (300 x 300 DPI)

A new Nuclear Electric Quadrupole Moment was determined for the ^{63}Cu nucleus by means of a linear regression analysis of experimental Nuclear Electric Quadrupole Constants against Electric Field Gradients obtained from relativistic calculations at several levels. The best result, given by the DC-CCSD-T approach, -198(10) mbarn, suggests a revision of the currently accepted standard value for this property.